Eur. Phys. J. D **46**, 1–8 (2008)
DOI: 10.1140/epjd/e2007-00270-x

THE EUROPEAN PHYSICAL JOURNAL D

Effect of strongly coupled plasma on the spectra of hydrogenlike carbon, aluminium and argon

S. Bhattacharyya[1], A.N. Sil[2,3,a], S. Fritzsche[4], and P.K. Mukherjee[3]

[1] Kandi Raj College, Kandi, Murshidabad, West Bengal 742 137, India
[2] Max Planck Institute for the Physics of Complex Systems, Nöthnitzer Str. 38, 01187 Dresden, Germany
[3] Indian Association for the Cultivation of Science, Jadavpur, Kolkata-700 032, India
[4] Universität Kassel, Institut für Physik, 34109 Kassel, Germany

Received 12 April 2007 / Received in final form 24 July 2007
Published online 21 September 2007 –

Abstract. A detailed study has been performed for estimating the orbital energies, positions and shifts of the Lyman lines of C^{5+}, Al^{12+} and Ar^{17+} under strongly coupled plasma with a view to understand such line positions and shifts obtained in laser produced plasma experiments. The effect of strongly coupled plasma has been treated within the Ion Sphere (IS) model. Both non-relativistic and relativistic methods have been used for estimating the spectral properties. Theoretical estimates with IS model of the plasma are in conformity with the results of laser plasma experiments on these highly stripped ions. The experimental data for the systems have also been compared with the theoretical estimates using Debye screening model of the plasma with spatial confinements which gives additional restrictions to the wave functions at finite boundaries.

PACS. 95.30.Qd Magnetohydrodynamics and plasmas – 52.27.Gr Strongly-coupled plasmas – 52.70.-m Plasma diagnostic techniques and instrumentation – 52.72.+v Laboratory studies of space- and astrophysical-plasma processes

1 Introduction

The spectral properties of atomic systems are modified considerably under external confinements [1–3]. Of particular interest, is the effect of a surrounding plasma of different coupling strengths Γ, defined as the ratio of average Coulomb potential energy between pairs of particles and their kinetic energy. For weakly coupled plasma $\Gamma < 1$ and one can apply the standard Debye screening model [4] in which the potential energy between charged particles is represented by a screened Coulomb potential. The condition $\Gamma \geq 1$ refers to strongly coupled plasma in which the potential energy function, though simple, is of completely different nature than in a Debye screening model [5]. Such plasma conditions prevail in, highly evolved stars, the interior of Jovian planets, explosive shock tubes, two dimensional states of electrons trapped in surface states of liquid helium, laser produced and inertial confinement fusion plasmas [5,6]. Recent experimental observations using laser produced plasmas [7–12] open up an interesting field for the theoretical investigations along this line. Such high density plasmas are of particular interest in astrophysics and inertial confinement fusion processes. The X-ray opacity of matter under stellar interior conditions and the X-ray diagnostics of ICF plasmas can be achieved from such a study [11]. Effect of dense plasma on the ionization potential, collision and photo absorption cross sections, fine structure splitting and spectral line shifts have been investigated earlier by Stewart and Pyatt [13], Rozsnai [14], Ray [15], Jung [16], Griem [17], Siedel et al. [18] and Skupski [19]. Applications of density functional approach along this line was reviewed by Gupta and Rajagopal [20].

In the current context, we will focus our attention to the experimental findings based on time and space resolved extreme ultraviolet spectra of carbon plasmas with 100 fs laser pulses [10], inertially confined laser imploded Ar plasma [11] and ultrashort laser produced Al plasma [12]. For such laser produced plasmas $\Gamma > 1$ and one can apply strongly coupled plasma model to investigate the spectral properties of isoelectronic ions of hydrogen. In this communication we would like to investigate in detail the effect of strongly coupled plasma on the Lyman lines of highly stripped carbon, aluminium and argon. Ion Sphere (IS) model of the plasma [5] has been utilized for such a study. Our motivation is to investigate how the simple IS model is effective in obtaining results which can be compared favourably with the experimentally observed values. In addition we would also like to investigate the applicability of the Debye plasma model with a spherical confinement on the spectral line positions and shifts of the Lyman lines under the laser plasma experimental

[a] e-mail: amar@mpipks-dresden.mpg.de

conditions [10–12] and to estimate the shifts in ionization potentials. Such studies have been done earlier for hydrogen [21,22] and helium like systems [23,24] to understand the behavior of the structural properties of one and two electron systems under weak as well as strongly coupled plasmas. A brief outline of the theory is given in Section 2 and a discussion of the results follow in Section 3.

2 Theory

In presence of an external plasma environment the potential energy is modified and the non-relativistic Hamiltonian of a hydrogen like atomic system [a.u. is used throughout] can be represented by

$$H_0 = -\frac{1}{2}\nabla^2 + V_{\mathit{eff}}(r) \tag{1}$$

where the structure of the one body effective potential depends on the type of the coupling of the plasma with the atomic charge cloud. For the relativistic treatment appropriate modification of the kinetic energy part of the Hamiltonian is done through the introduction of the Dirac operators. Once the form of the Hamiltonian is known the effect of the external plasma can be taken care of by using a suitable form of the effective one particle potential. Currently we are interested in the case of strongly coupled plasma for which $\Gamma \geq 1$. For such a case the model which is usually referred to as the Ion Sphere (IS) model [5] has been adopted here for the estimation of line shifts. Physically the IS model assumes a smeared out uniform electron density distribution within a sphere and zero density outside [5,13]. In this model for the case of a homogeneous one component plasma surrounding an ion of nuclear charge Z having one valence electron like hydrogenic ions described here, one can define a sphere of radius R (usually referred to as the Wigner-Seitz radius) such that the plasma electrons contained in this sphere together with the valance electron completely neutralize the central positive charge; thus maintaining the overall charge neutrality of the system within this sphere [5,13,20]. Since the total charge within the Wigner-Seitz sphere is important one can use a volume averaged density for performing the calculation as existing in literature [13,14]. In such a situation the Wigner-Seitz radius R can be represented by

$$R = \left[\frac{(Z-1)}{\frac{4}{3}\pi n}\right]^{\frac{1}{3}} \tag{2}$$

where n is the average electron density within the sphere.

The expression for the potential can easily be obtained from classical electrostatics as

$$V_{\mathit{eff}}(r) = -\frac{Z}{r} + \frac{(Z-1)}{2R}\left[3 - \left(\frac{r}{R}\right)^2\right]. \tag{3}$$

In order to analyze the energy of the system for different coupling strengths of the plasma reflected in R, one has to solve the appropriate Schrödinger equation

$$H_0\psi = E_0\psi \tag{4}$$

subject to the normalization constant

$$\langle\psi|\psi\rangle = 1. \tag{5}$$

For the relativistic case the corresponding Dirac equation is to be solved. It is assumed that no electron current takes place at the boundary surface defined by the Wigner-Seitz radius R and the wave function is assumed to satisfy the boundary condition Stewart [13], Rozsnai [14], and Skupski [19]

$$\psi(r) = 0 \qquad \text{at} \quad r = R. \tag{6}$$

Other boundary conditions involving vanishing of the first derivative of the orbital at the boundary can also be adopted as was done by Rozsnai [14]. However, we have taken the boundary condition given by equation (6) for computational simplicity. Such conditions can always be satisfied by choosing the basis sets appropriately. We represent the radial part of the orbital

$$\psi(r) = (R-r)\chi(r) \tag{7}$$

where $\chi(r)$ is a linear combination of Slater type orbitals (STO)

$$\chi(r) = \sum_i C_i r^{n_i} e^{-\rho_i r}. \tag{8}$$

The analytical solution of hydrogen like problem in a plasma is difficult. We adopt the basis set expansion technique for obtaining the energy of the ground state in a plasma environment for the non relativistic calculation. The non linear parameters n_i and ρ_i for the ground orbital are preassigned from physical considerations and the linear coefficients are determined from the solution of the generalized eigenvalue equation

$$\mathbf{H}_0\,\mathbf{C} = E_0\mathbf{S}\,\mathbf{C} \tag{9}$$

where $\mathbf{H}_0$ and $\mathbf{S}$ are the Hamiltonian and the overlap matrices with respect to the basis sets and $\mathbf{C}$ is the coefficient vector. Solution of equation (9) yields the ground state energy and the linear coefficients at different plasma coupling strengths which are functions of the plasma parameters. All the integrals are to be evaluated at finite domain radius R. The appropriate integral package has been developed. For the relativistic case a numerical evaluation of the energies is sought using Dirac Hamiltonian and the standard relativistic program package RATIP as developed by Fritzsche et al. [25].

In addition to evaluation of the ground state energies at different plasma coupling strengths we apply an external time dependent perturbation [21–24] for probing the low lying excited states of the system. The transition energies and excited state wave functions have been calculated using linear response theory under such a perturbation [21–24]. The procedure yields the spectral line positions and other excitation properties under the plasma environment.

Table 1. Relativistic and non-relativistic transition energy of Al^{12+} for different Ion-Sphere (IS) radius.

Ion-sphere radius (a.u.)	Plasma density n_e/c.c.	Orb Ener (a.u.) Rel	Orb Ener (a.u.) Non-Rel	Transition scheme	Transition energy (a.u.) Rel	Transition energy (a.u.) Non-Rel	Energy shift (eV) Rel	Energy shift (eV) Non-Rel
∞		84.69	84.50	$1s \rightarrow 2p$	63.53747	63.37500		
				$\rightarrow 3p$	75.28958	75.11111		
				$\rightarrow 4p$	79.40327	79.21875		
9.9	1.99(+22)	82.8729	82.6819	$1s \rightarrow 2p$	63.53715	63.37401	0.0087	0.0269
				$\rightarrow 3p$	75.28855	75.10482	0.0280	0.1709
				$\rightarrow 4p$	79.38251	79.19697	0.5649	0.5927
5.7822	1.0(+23)	81.5785	81.3876	$1s \rightarrow 2p$	63.53319	63.37003	0.1165	0.1352
				$\rightarrow 3p$	75.26206	75.09233	0.7489	0.5108
				$\rightarrow 4p$	79.29516	79.10701	2.9418	3.0406
3.38146	5.0(+23)	79.3706	79.1796	$1s \rightarrow 2p$	63.51337	63.35014	0.6558	0.6765
				$\rightarrow 3p$	75.12798	74.98010	4.3974	3.5647
				$\rightarrow 4p$	78.86261	78.70955	14.7121	13.8540
3.18207	6.0(+23)	79.0376	78.8467	$1s \rightarrow 2p$	63.50841	63.34516	0.7908	0.8120
				$\rightarrow 3p$	75.09388	74.94203	5.3253	4.6006
				$\rightarrow 4p$	78.75720	78.66120	17.5805	15.1717
3.0227	7.0(+23)	78.7399	78.5489	$1s \rightarrow 2p$	63.50344	63.34018	0.9260	0.9475
				$\rightarrow 3p$	75.05951	74.90371	6.2605	5.6434
2.89111	8.0(+23)	78.4694	78.2784	$1s \rightarrow 2p$	63.49847	63.33519	1.0612	1.0833
				$\rightarrow 3p$	75.02489	74.86516	7.2026	6.6924
2.7798	9.0(+23)	78.2206	78.0297	$1s \rightarrow 2p$	63.49349	63.33019	1.1968	1.2193
				$\rightarrow 3p$	74.98993	74.82618	8.1539	7.7531
2.68386	1.0(+24)	77.9897	77.7987	$1s \rightarrow 2p$	63.48851	63.32519	1.3323	1.3554
				$\rightarrow 3p$	74.95463	74.78648	9.1145	8.8334
2.13018	2.0(+24)	76.2519	76.0610	$1s \rightarrow 2p$	63.43847	63.27495	2.6939	2.7225
				$\rightarrow 3p$	74.58295	74.31376	19.2284	21.6967
1.97749	2.5(+24)	75.6022	75.4113	$1s \rightarrow 2p$	63.41328	63.24965	3.3794	3.4109
				$\rightarrow 3p$	74.38536	74.03433	24.6051	29.3004
1.86089	3.0(+24)	75.0346	74.8437	$1s \rightarrow 2p$	63.38798	63.22420	4.0678	4.1035
				$\rightarrow 3p$	74.18693	73.75165	30.0046	36.9925
1.76768	3.5(+24)	74.5273	74.3364	$1s \rightarrow 2p$	63.36256	63.19856	4.7595	4.8012
				$\rightarrow 3p$	73.98516	73.47956	35.4951	44.3965
1.4770	6.0(24)	72.5370	72.3461	$1s \rightarrow 2p$	63.23364	63.06557	8.2676	8.4800
1.3419	8.0(24)	71.3210	71.1306	$1s \rightarrow 2p$	63.12816	62.94926	11.1379	11.5850
1.2457	1.0(25)	70.2961	70.1059	$1s \rightarrow 2p$	63.02080	62.82014	14.0593	15.0985

To be more specific we apply a harmonic perturbation on the system

$$H'(\mathbf{r},t) = g(\mathbf{r})e^{-i\omega t} + g^{\dagger}(\mathbf{r})e^{i\omega t} \tag{10}$$

where $g(\mathbf{r})$ is an one particle perturbation operator. The angular part of the perturbation operator is so chosen as to get a dipolar excitation from the ground state enabling us to compare the laser spectroscopic data. The external perturbation changes the ground state wave function ψ to the perturbed function ϕ. The first order perturbation correction to the ground state wave function oscillates harmonically and its spatial part can be evaluated through the optimization of a standard variational functional [26]

$$J(\phi) = \frac{1}{T}\int_0^T dt \frac{\langle\phi|H_0 + H' - i\frac{\partial}{\partial t}|\phi\rangle}{\langle\phi|\phi\rangle} \tag{11}$$

with

$$\delta J(\phi) = 0. \tag{12}$$

The optimization is carried out with respect to linear variation parameters introduced in the first order correction to the ground state function ψ. The procedural details have been given elsewhere [21–24]. The basis sets for the perturbed functions are similar to that given by equations (7) and (8) with different linear and non linear parameters. The functional has poles at certain frequency ω, the positions of which indicate the singly excited states of the system. One can extract the transition properties from a study of the pole positions [21]. For the relativistic case RATIP package generates the relevant excitation properties directly [25]. A discussion of the results is given in the next section.

3 Results and discussions

The effect of strongly coupled plasma on the orbital energy and low lying excited states of C^{5+}, Al^{12+} and Ar^{17+} has been analyzed in details using IS model within non relativistic as well as relativistic theory. We use this model

Table 2. Relativistic and non-relativistic transition energy of Al^{12+} for different Debye screening parameter and box radius.

Ion	Plasma density (/c.c.)	Temp. (eV)	Debye para (a.u.)	Debye Sh Rad (a.u.)	Orbital energy $-E$ (a.u.)		Transition scheme	Transition energy (a.u.)		Energy shift (eV)	
					Rel	Non-Rel		Rel	Non-Rel	Rel	Non-Rel
Al^{12+}	1.0(22)	300	0.154	6.50328	82.7066	82.5156	$1s \rightarrow 2p$	63.49789	63.33468	1.0770	1.0972
							$3p$	75.17195	74.99568	3.2009	3.1410
							$4p$	79.17590	78.98747	6.1871	6.2935
	1.5(22)	300	0.188	5.30991	82.2731	82.0823	$1s \rightarrow 2p$	63.47852	63.31529	1.6041	1.6248
							$3p$	75.11382	74.95165	4.7827	4.3391
							$4p$	79.07184	78.88048	9.0187	9.2048
	2.0(22)	300	0.217	4.59852	81.9048	81.7139	$1s \rightarrow 2p$	63.45912	63.29586	2.1320	2.1535
							$3p$	75.05604	74.90643	6.3550	5.5696
							$4p$	78.97013	78.77558	11.7863	12.0593
	2.5(22)	300	0.243	4.11304	81.5756	81.3847	$1s \rightarrow 2p$	63.43951	63.27621	2.6656	2.6882
							$3p$	74.99892	74.85465	7.9093	6.9786
							$4p$	78.86956	78.67419	14.5230	14.8182
	3.0(22)	300	0.266	3.75467	81.2852	81.0944	$1s \rightarrow 2p$	63.42043	63.25709	3.1848	3.2085
							$3p$	74.94271	74.79863	9.4388	8.5030
							$4p$	78.77459	78.58558	17.1073	17.2294
	3.5(22)	300	0.288	3.47615	81.0081	80.8173	$1s \rightarrow 2p$	63.40068	63.23729	3.7222	3.7473
							$3p$	74.88485	74.73743	11.0133	10.1684
							$4p$	78.67940	78.50974	19.6975	19.2932
	4.0(22)	300	0.308	3.25164	80.7568	80.5661	$1s \rightarrow 2p$	63.38146	63.21803	4.2453	4.2714
							$3p$	74.82883	74.67665	12.5377	11.8223
							$4p$	78.58756	78.45786	22.1966	20.7049
	4.5(22)	300	0.326	3.06568	80.5311	80.3404	$1s \rightarrow 2p$	63.36315	63.19967	4.7435	4.7710
							$3p$	74.77574	74.61846	13.9823	13.4057
							$4p$	78.51635	78.43443	24.1343	21.3424
	5.0(22)	300	0.344	2.90836	80.3059	80.1152	$1s \rightarrow 2p$	63.34388	63.18036	5.2679	5.2964
							$3p$	74.72022	74.55784	15.4931	15.0553
							$4p$	78.45252	78.43180	25.8712	21.4140

as it is simple and expected to produce results in reasonable agreement with the experimental data. The particular ions have been chosen here as laser produced plasma experiments in such systems exist [10–12] and spectral lines of Lyman series originating in plasma environments have been reported. Our aim is to see the reliability of the IS model of the plasma in predicting the experimentally observed lines of the Lyman series. The shifts can always be estimated from the free line positions. The orbital energies for different plasma coupling strengths have been obtained from the solution of the generalized eigenvalue equation (9) with respect to a limited basis set composed of linear combination of STO's. For C^{5+} ion we have chosen only a two parameter representation for the ground orbital and its reliability has been tested by comparing the eigen energy for the free systems. For Al^{12+} and Ar^{17+} we have chosen four parameter representation for the same. To study the excitation energies and transition wavelengths under plasma we used a twelve parameter representation of the first order perturbed orbitals for C^{5+} while an 8 parameters representation was adopted for Al^{12+} and Ar^{17+}. For the case of Al^{12+} and Ar^{17+} the results for our detailed investigations using IS model with different electron densities have been displayed in Tables 1 and 3. We have considered the behavior of the ground state orbital energy and the transition energy to first three dipole allowed excited states $2p$, $3p$ and $4p$. The energy shifts have been calculated for Al^{12+} while for Ar^{17+}, the wavelengths for the free as well as those in presence of plasma have been reported. This is because the data on the laser produced experiments on plasma for Al^{12+} [12] and Ar^{17+} [11] have been given accordingly. The other model which exists in literature is the so-called Debye model [4]. Here the effect due to the surrounding plasma is given by a screened Coulomb potential. In order to have an idea about how the results from Debye model compare with those from IS model as well as experimental data, we have computed the energy levels and other properties using Debye model with spherical confinement, the radius of confinement being the inverse of the Debye screening parameter which determines the sphere of influence. Here the effective potential is given by [4]

$$V_{eff}(r) = -\frac{Ze^{-\mu r}}{r} \tag{13}$$

where Z is the nuclear charge and μ is the Debye screening parameter given by

$$\mu = \left[\frac{4\pi(1+Z)n}{\kappa T}\right]^{\frac{1}{2}} \tag{14}$$

Table 3. Relativistic and non-relativistic transition energy of Ar^{17+} for different Ion-Sphere (IS) radius.

Ion	Plasma density (/c.c.)	IS radius (a.u.)	Orbital energy $-E$ (a.u.)		Transition scheme	Transition energy (a.u.)		Transition wave length (Å)	
			Rel	Non-Rel		Rel	Non-Rel	Rel	Non-Rel
Ar^{17+}	9.54(20)	30.0	161.8549	161.1500	$1s \rightarrow 2p$	122.10220	121.49997	3.7305	3.7490
					$3p$	144.66130	143.99982	3.1488	3.1633
					$4p$	152.56180	151.87442	2.9857	2.9992
	2.58(22)	10.0	160.1549	159.4500	$1s \rightarrow 2p$	122.10153	121.49929	3.7306	3.7491
					$3p$	144.65685	143.99535	3.1489	3.1633
					$4p$	152.54681	151.86477	2.9860	2.9994
	1.0(23)	6.4941	158.7785	158.0736	$1s \rightarrow 2p$	122.09966	121.49741	3.7306	3.7491
					$3p$	144.64459	143.98306	3.1492	3.1636
					$4p$	152.50553	151.81798	2.9868	3.0004
	2.0(23)	5.1543	157.7581	157.0533	$1s \rightarrow 2p$	122.09709	121.49482	3.7307	3.7492
					$3p$	144.62769	143.96644	3.1495	3.1640
					$4p$	152.44872	151.75973	2.9879	3.0015
	3.0(23)	4.5027	157.0425	156.3376	$1s \rightarrow 2p$	122.09452	121.49223	3.7308	3.7493
					$3p$	144.61075	143.95059	3.1499	3.1643
					$4p$	152.39194	151.70093	2.9891	3.0027
	4.0(23)	4.0190	156.3612	155.7680	$1s \rightarrow 2p$	122.09138	121.48964	3.7309	3.7494
					$3p$	144.59007	143.93565	3.1503	3.1647
					$4p$	152.32277	151.62842	2.9904	3.0041
	5.0(23)	3.7978	155.9918	155.2869	$1s \rightarrow 2p$	122.08937	121.48705	3.7309	3.7494
					$3p$	144.57679	143.92126	3.1506	3.1650
					$4p$	152.27847	151.58148	2.9913	3.0050
	6.0(23)	3.5738	155.5713	154.8665	$1s \rightarrow 2p$	122.08680	121.48447	3.7310	3.7495
					$3p$	144.55975	143.90649	3.1510	3.1653
					$4p$	152.22179	151.52097	2.9924	3.0062
	7.0(23)	3.3948	155.1954	154.4906	$1s \rightarrow 2p$	122.08422	121.48187	3.7311	3.7496
					$3p$	144.54269	143.89068	3.1514	3.1657
					$4p$	152.16513	151.46022	2.9935	3.0074
	8.0(23)	3.2470	154.8538	154.1490	$1s \rightarrow 2p$	122.08165	121.47928	3.7312	3.7497
					$3p$	144.52559	143.87384	3.1517	3.1660
					$4p$	152.10852	151.39962	2.9946	3.0086
	9.0(23)	3.1220	154.5396	153.8348	$1s \rightarrow 2p$	122.07908	121.47669	3.7313	3.7498
					$3p$	144.50846	143.85638	3.1521	3.1664
					$4p$	152.05193	151.33965	2.9957	3.0098
	1.0(24)	3.0143	154.2480	153.5431	$1s \rightarrow 2p$	122.07650	121.47410	3.7313	3.7498
					$3p$	144.49129	143.83861	3.1525	3.1668
					$4p$	151.99539	151.28082	2.9969	3.0110
	1.5(24)	2.6332	153.0251	152.3203	$1s \rightarrow 2p$	122.06361	121.46113	3.7317	3.7502
					$3p$	144.40493	143.74921	3.1544	3.1688
					$4p$	151.71395	151.01987	3.0024	3.0162
	1.8(24)	2.4780	152.4192	151.7144	$1s \rightarrow 2p$	122.05588	121.45334	3.7320	3.7505
					$3p$	144.35266	143.69573	3.1555	3.1699
					$4p$	151.54573	150.90012	3.0057	3.0186
	2.0(24)	2.3924	152.0519	151.3471	$1s \rightarrow 2p$	122.05071	121.44814	3.7321	3.7506
					$3p$	144.31763	143.66004	3.1563	3.1707
					$4p$	151.43565	150.83746	3.0079	3.0199
	2.5(24)	2.2209	151.2303	150.5256	$1s \rightarrow 2p$	122.03780	121.43514	3.7325	3.7510
					$3p$	144.22930	143.57026	3.1582	3.1727
					$4p$	151.15811	150.73922	3.0135	3.0218

μ is a function of the temperature T and number density n of the plasma electrons. One can simulate a large number of plasma conditions by properly choosing n and T. Using the potential function given by equation (13) with a given parameter μ, one can proceed in the same way as is being done in the strongly coupled plasma model to study the behavior of orbital energies and excitation properties. In such calculations we have chosen the plasma temperature T as reported in the experimental papers [11,12] and varies the electron density n to get the screening parameters μ. For each μ value we have chosen the radius of confinement as $R = \frac{1}{\mu}$ which effectively gives the Debye sphere of influence. The spatial confinement with respect to the Debye radius is incorporated in the numerical

Table 4. Relativistic and non-relativistic transition energy of Ar^{17+} for different Debye screening parameter and box radius.

Ion	Plasma density (/c.c.)	Temp (eV)	Debye para (a.u.)	Debye radius (a.u.)	Orbital energy $-E$ (a.u.)		Tran. sch.	Transition energy (a.u.)		Transition wave length (Å)	
					Rel	Nol-Rel		Rel	Nol-Rel	Rel	Nol-Rel
Ar^{17+}	1.0(23)	1000	0.3103	3.2230	157.1904	156.4865	$1s \rightarrow 2p$	121.94107	121.33840	3.7355	3.7540
							$3p$	144.17601	143.52411	3.1594	3.1737
							$4p$	151.67941		3.0031	
	5.0(23)	1000	0.6938	1.4414	150.5664	149.8640	$1s \rightarrow 2p$	121.33281	120.72769	3.7542	3.7730
							$3p$	142.49773	141.51795	3.1966	3.2187
							$4p$	150.25318		3.0316	
	1.0(24)	1000	0.9812	1.0192	145.7360	145.0367	$1s \rightarrow 2p$	120.61125	119.98983	3.7767	3.7962
							$3p$	141.17721	138.52859	3.2265	3.2882
	5.0(24)	1000	2.1939	0.4558	126.5337	125.8566	$1s \rightarrow 2p$	116.71007	111.28980	3.9029	4.0930

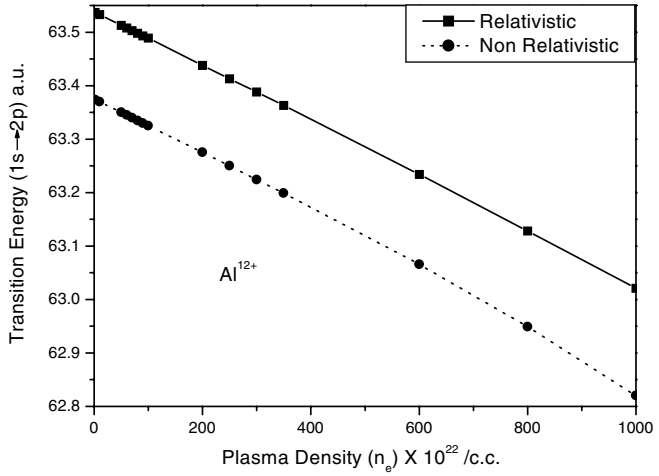

Fig. 1. Plot of the relativistic and non relativistic transition energy ($1s \rightarrow 2p$) (a.u.) obtained by using IS model against plasma electron density (/cc) for Al^{12+}.

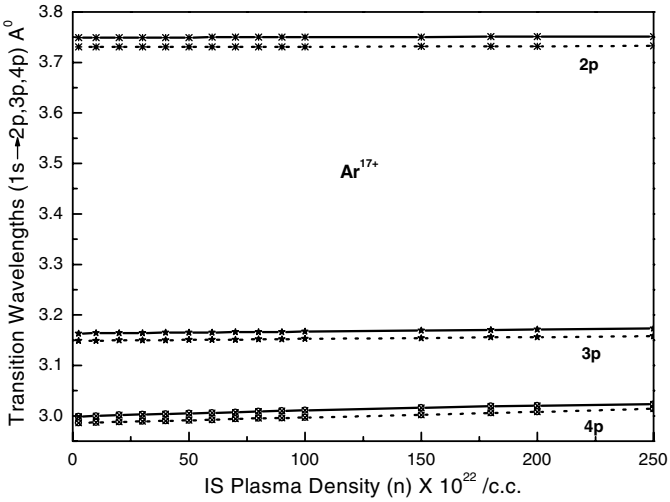

Fig. 2. Plot of the relativistic (dotted line with symbols) as well as non relativistic transition (solid line with symbols) wavelength ($1s \rightarrow 2p$, $3p$, $4p$) (Å) obtained by using IS model against plasma electron density (/cc) for Ar^{17+}.

calculations in exactly the same way as is being done for the Ion Sphere (IS) model. Such results have been displayed in Tables 2 and 4 for the respective cases of Al^{12+} and Ar^{17+}. The number of parameters for the ground and excited state functions are identical in the Debye plasma and in the IS models. In Tables 1 to 4 the transition energies from the $1s \rightarrow 2p$, $3p$ and $4p$ states have been reported for the cases only in which the excited state is bound. As soon as the transition energy exceeds that of the ionization energy for increased plasma strength, it goes in the continuum and such cases have not been displayed in the tables. Experimental shift for the Lyman α (Ly_α) line for Al^{12+} with estimated electron density $n \sim (5{-}10) \times 10^{23}$/cc and temperature $T \sim 300$ eV is given by 3.7 ± 0.7 eV [12]. Our calculation using IS model at $n = 2.5 \times 10^{24}$/cc yields a value 3.41 eV whereas a quantum mechanical calculations of Nguyen et al. [27] based on collision theory yields a value 3.5 eV at $n = 8 \times 10^{23}$/cc and $T \sim 300$ eV.

Figure 1 shows the general trend of the transition energy $1s \rightarrow 2p$ for Al^{12+} against the Ion Sphere radius R with non relativistic and relativistic models. For the relativistic case weighted average of the $p_{\frac{3}{2}}$ and $p_{\frac{1}{2}}$ state energies have been reported all throughout. It appears that the relativistic results differ only at higher plasma electron densities. In Figure 2 we plotted the non relativistic and relativistic transition wavelengths $1s \rightarrow 2p$, $3p$ and $4p$ against IS plasma density for Ar^{17+}. The relativistic effects are little more pronounced here as the nuclear charge Z is larger. Figure 3 displays a comparison of our calculated results for the transition wavelengths for Ar^{17+} using non relativistic as well as relativistic methods within Ion Sphere (IS) model and spatially confined Debye screening model with the laser plasma experimental data. The wavelengths for the $1s \rightarrow 2p$, $3p$, $4p$ transitions as obtained from an analysis of the experimental data [11] are 3.7494, 3.2394 and 2.9927 Å respectively. They are in reasonable agreement with the calculated theoretical results using IS model with electron density 10^{24}/cc. The laser plasma experiment by Nantel et al. [10] yields data on hydrogen and helium like spectra of C under strong

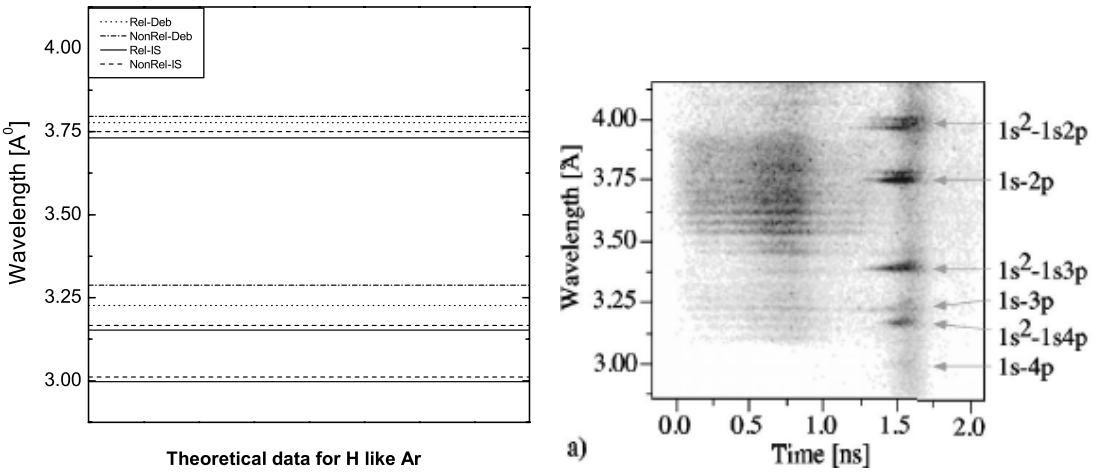

Fig. 3. Comparison between the experimental results and that obtained theoretically by using Ion Sphere as well as Debye plasma model for $1s \rightarrow 2p$, $3p$, $4p$ transition wavelength (Å) of Ar^{17+}. We have taken same plasma temperature ($T = 1000$ eV) and density ($n_e = 10^{24}$/c.c.) as was in the experiment. The experimental figure has been taken from reference [11].

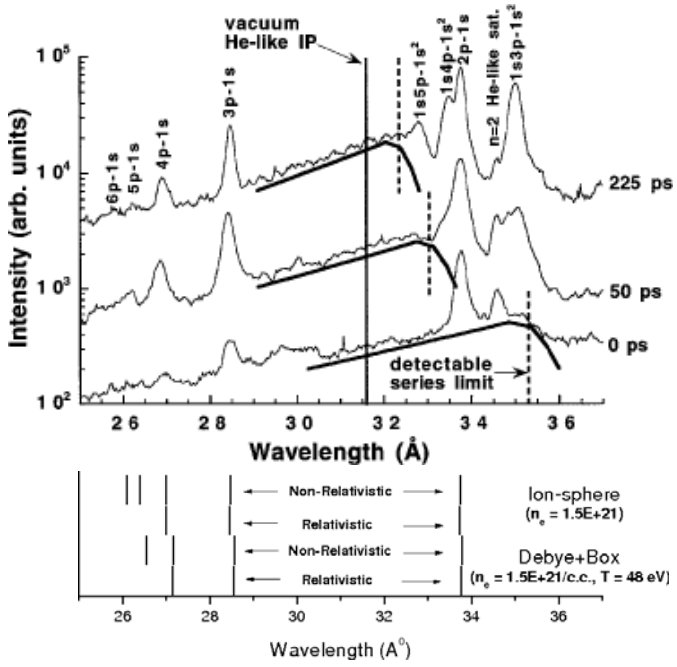

Fig. 4. Comparison between the experimental results (C^{4+} and C^{5+}) and that obtained theoretically by using Ion Sphere as well as Debye plasma model for $1s \rightarrow 2p$, $3p$, $4p$, $5p$, $6p$ transition wavelength (Å) of hydrogen like carbon. The experimental figure has been taken from reference [10].

plasma with estimated density of $n = 1.5 \times 10^{21}$/cc and temperature 48 eV. We have performed non relativistic and relativistic estimates of the positions of Lyman lines of C^{5+} using the Ion Sphere (IS) model at experimental density and spatially confined Debye plasma model at the same density and temperature. In Figure 4 we displayed our results along with those obtained by Nantel et al. [10]. We observed very reasonable fitting with the experimental lines positions for the Lyman transitions $1s \rightarrow 2p$, $3p$, $4p$, $5p$ and $6p$ for which the respective wavelengths as obtained from an analysis of the line profiles are 33.7491, 28.4667, 26.8791, 26.2104 and 25.7380 in Å. It appears that with IS model non relativistic and relativistic estimates at $n = 1.5 \times 10^{21}$/cc and temperature 48 eV agree well with experimental data, while there are little variations with confined Debye plasma model. This is reflected in Table 5, where we compare the experimental data with our theoretical estimates for C^{5+} and Ar^{17+} using non relativistic as well relativistic models. Since we are concerned with hydrogenic spectra in which no electron correlation effect is present, our theoretical results should be accurate enough to be compared with experimental data. The accuracy of our results could be assessed from a comparison with the energy levels for the free system for which we get exact agreement. The accuracy of the experimental data is difficult to assess as most of the authors do not furnish the error bars. The experiments deal with complex situation with plasma in non LTE where density and temperature evolve. The experimental condition assumes a simulated temperature and density which has a range. We have performed the calculations with the reported density and temperature and tried to obtain the best fit with the experiments.

4 Conclusion

From the analysis of the calculated data by using IS and Debye models one can conclude that IS model, though simple, yields very reasonable theoretical estimates of spectral line positions and shifts of the spectral lines obtained from laser produced plasmas. It can be a viable method for the understanding of the experimental observations on strongly coupled plasmas obtained in laboratory and astrophysics.

Table 5. Comparison between experimental and theoretical results of relativistic and non-relativistic transition wavelength of C^{5+} and Ar^{17+}. The experimental data have been extracted from Figure 1 of reference [10] and Figure 2a of reference [11] for C^{5+} and Ar^{17+} respectively.

Excitation	Transition wavelength (Å)				
	IS model results		Debye model results		Experimental results
	Non-relativistic	Relativistic	Non-relativistic	Relativistic	
		C^{5+}			
$1s \rightarrow 2p$	33.7422	33.7238	33.7878	33.7693	33.7491
$1s \rightarrow 3p$	28.4733	28.4589	28.5693	28.5546	28.4667
$1s \rightarrow 4p$	27.0055	26.9918	27.1597	27.1427	26.8791
$1s \rightarrow 5p$	26.3906		26.5488		26.2104
$1s \rightarrow 6p$	26.0926		25.9557		25.7380
		Ar^{17+}			
$1s \rightarrow 2p$	3.7498	3.7311	3.7962	3.7767	3.7494
$1s \rightarrow 3p$	3.1668	3.1525	3.2882	3.2265	3.2394
$1s \rightarrow 4p$	3.0110	2.9969			2.9927

The authors (PKM and SF) are thankful to AvH foundation for financial assistance towards mutual visits of Indian and German scientists. The financial assistance from the Department of Science and Technology (DST), Govt. of India under research grant no. SR/S2/LOP-05/2005 is gratefully acknowledged.

References

1. B. Tabbert, H. Günther, G. zu Putlitz, J. Low. Temp. Phys. **109**, 653 (1997)
2. W. Jaskolski, Phys. Rep. **271**, 1 (1996)
3. J.P. Connerade, V.K. Dolmatov, P.A. Lakshmi, J. Phys. B, At. Mol. Opt. Phys. **33**, 251 (2000)
4. A.I. Akhiezer, I.A. Akhiezer, R.A. Polovin, A.G. Sitenko, K.N. Stepanov, *Plasma Electrodynamics*, *linear response theory* (Pergamon, Oxford, 1975), Vol. 1
5. S. Ichimaru, Rev. Mod. Phys. **54**, 1017 (1982)
6. B.A. Hammel, C.J. Keane, M.D. Cable, D.R. Kania, J.D. Kilkenny, R.W. Lee, R. Pasha, Phys. Rev. Lett. **70**, 1263 (1993)
7. L. DaSilva, A. Ng, B.K. Godwal, G. Chiu, F. Cottet, M.C. Richardson, P.A. Jaanimagi, Phys. Rev. Lett. **62**, 1623 (1989); A. Djaoui et al., Plasma Phys. Contr. Fus. **31**, 111 (1989)
8. E. Leboucher-Dalimier, A. Poquerusse, P. Angelo, I. Gharbi, H. Derfoul, J. Quant. Spectrosc. Radiat. Transfer **51**, 187 (1994)
9. J. Workman, M. Nantel, A. Maksimchuk, D. Umstadter, Appl. Phys. Lett. **70**, 312 (1997)
10. M. Nantel, G. Ma, S. Gu, C.Y. Cote, J. Itatani, D. Umstadter, Phys. Rev. Lett. **80**, 4442 (1998)
11. N.C. Woolsey, B.A. Hammel, C.J. Keane, C.A. Back, J.C. Moreno, J.K. Nash, A. Calisti, C. Mosse, R. Stamm, B. Talin, A. Asfaw, L.S. Klein, R.W. Lee, Phys. Rev. E **57**, 4650 (1998)
12. A. Saemann, K. Eidmann, I.E. Golovkin, R.C. Mancini, E. Andersson, E. Forster, K. Witte, Phys. Rev. Lett. **82**, 4843 (1999)
13. J.C. Stewart Jr, K.D. Pyatt, Astrophys. J. **144**, 1203 (1966)
14. B.F. Rozsnyai, Phys. Rev. A **43**, 3035 (1991)
15. D. Ray, Phys. Rev. E **62**, 4126 (2000)
16. Y.D. Jung, Eur. Phys. J. D **7**, 249 (1999), and references therein
17. H.R. Griem, Phys. Rev. A **15**, 2943 (1988); H.R. Griem *Spectral Line Broadening by Plasmas* (Academic Press, New York, 1974)
18. J. Seidel, S. Arndt, W.D. Kraeft, Phys. Rev. E **52**, 5387 (1995)
19. S. Skupski, Phys. Rev. A **21**, 1316 (1980)
20. U. Gupta, A.K. Rajagopal, Phys. Rept. **87**, 259 (1982)
21. B. Saha, P.K. Mukherjee, G.H.F. Diercksen, Astron. Astrophys. **396**, 337 (2002)
22. A.N. Sil, B. Saha, P.K. Mukherjee, Int. J. Quantum Chem. **104**, 903 (2005)
23. B. Saha, P.K. Mukherjee, D. Bielinska-Waz, Jacek Karwowski, J. Quant. Spectrosc. Radiat. Transfer **92**, 1, (2005); **78**, 131 (2003)
24. A.N. Sil, P.K. Mukherjee, Int. J. Quantum Chem. **106**, 465 (2006)
25. S. Fritzsche, J. Electr. Spec. Rel. Phenom. **114-116**, 1155 (2001); S. Fritzsche, Phys. Scr. **T100**, 37 (2002)
26. P.O. Löwdin, P.K. Mukherjee, Chem. Phys. Lett. **14**, 1 (1972)
27. H. Nguyen, M. Koenig, D. Benredjem, M. Caby, G. Coulaud, Phys. Rev. A **33**, 1279 (1986)